

Self-Reversal in Hydrogen Lyman- α Line Profile

Motoshi GOTO and Shigeru MORITA

National Institute for Fusion Science, Toki 509-5292, Japan

(Received 8 December 2009 / Accepted 20 March 2010)

A detailed spectral profile of the Lyman- α line of neutral hydrogen, i.e., the transition from $n = 2$ to the ground state, where n is the principal quantum number, was measured with a vacuum ultraviolet spectrometer for the plasma in the Large Helical Device. Self-reversal was observed in the spectral profile when the plasma density was increased with repetitive injection of hydrogen pellets. A one-dimensional radiation transport model was used for creating the Lyman- α spectral profile, for which an emission and absorption medium with a slab geometry and constant plasma parameters were assumed. The population density of the $n = 2$ level generally has a peaked spatial profile even with constant ground state density because of the reabsorption effect which is essential for the emergence of self-reversal in the spectral profile. We used the $n = 2$ level population distribution in the medium by Molisch *et al.* [*Radiation Trapping in Atomic Vapours*, Oxford University, Oxford, 1998] and evaluated the Lyman- α spectral profile as a function of the optical thickness. The observed line profile was found to be well fitted, for example, with a ground state density of $5.2 \times 10^{18} \text{ m}^{-3}$ and a medium thickness of 10 cm when a Lorentzian profile having a full width at half maximum of 0.0018 nm is adopted for the emission and absorption coefficients.

© 2010 The Japan Society of Plasma Science and Nuclear Fusion Research

Keywords: Lyman- α , self-reversal, reabsorption effect, LHD, internal diffusion barrier

DOI: 10.1585/pfr.5.S2089

1. Introduction

Self-reversal in the hydrogen Lyman- α line profile has been observed for high density discharges in the Large Helical Device (LHD) [1]. Most of the hydrogen may exist as molecules in the vacuum region outside the plasma. When these molecules penetrate into the plasma, they are dissociated to yield atoms owing to electron collisions, and these atoms are then ionized at a certain penetration length called the ionization length.

Since the ionization length of atomic hydrogen is known to be several centimeters in the LHD plasma [2], the Lyman- α line is emitted in a narrow layer at the plasma boundary. When the atom density is high, the reabsorption effect in the atom layer could be significant, and self-reversal may be observed. The occurrence of self-reversal suggests that this atom layer has a considerably large optical thickness for the Lyman- α line.

Conventionally, the hydrogen atom density has been evaluated from the Balmer- α line intensity, which represents the $n = 3$ level density, where n stands for the principal quantum number. However, since the ratio of the excited level density to the ground state density depends on the electron temperature T_e and the electron density n_e , derivation of the ground state atom density from the Balmer- α line intensity requires an appropriate collisional-radiative model, as well as accurate T_e and n_e values at the location of the emission.

On the other hand, since reabsorption of the Lyman- α

line is caused by ground state atoms, the magnitude of the reabsorption effect should directly reflect the ground state atom density. Here, self-reversal in the Lyman- α spectral profile is quantitatively evaluated on the basis of the radiation transport model, and a quantity that corresponds to the product of the ground state atom density and the thickness of the atom layer is determined.

The neutral pressure outside the confinement region is considered to be a key parameter for the formation of an internal diffusion barrier (IDB) [3], which has recently been studied intensively in LHD. Therefore, the present study is important.

2. Experiment

Spectral profile measurement is carried out with a 3 m vacuum ultraviolet spectrometer having a grating with 1200 grooves/mm [4]. Second order diffracted light (243.132 nm) is used for the measurement of the Lyman- α line. The reciprocal linear dispersion is 0.142 nm/mm at this wavelength. The instrumental function is well approximated by a Gaussian profile with a half width of 0.0033 nm. The spectrometer is equipped with a spatial resolution slit, which allows recording of chord-resolved spectra with a charge coupled device (CCD) detector [4].

The observation is carried out for a horizontally elongated poloidal cross section of the plasma. A detailed description is available in Ref. [4]. The width of the spatial resolution slit and the binning pattern on the CCD detector for data acquisition are arranged so that the entire cross

author's e-mail: goto@nifs.ac.jp

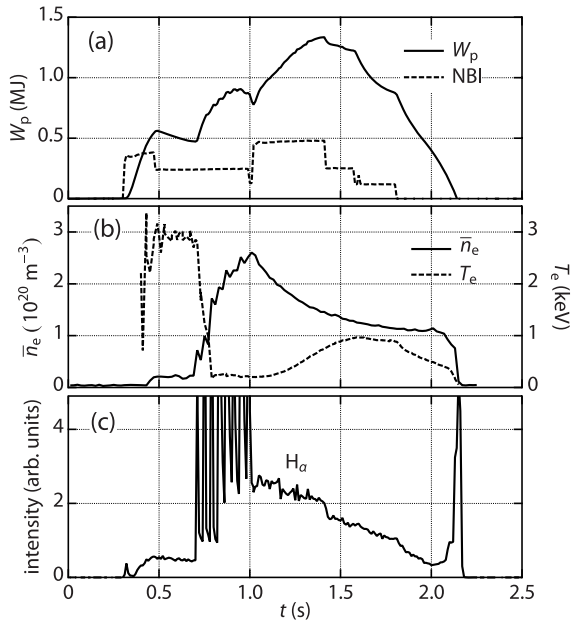


Fig. 1 Temporal development of discharge for the present measurement: (a) stored energy (solid line; W_p) and neutral beam power (dashed line; NBI) in arbitrary units, (b) line-averaged electron density (solid line; \bar{n}_e) and central electron temperature (dashed line; T_e), and (c) Balmer- α line intensity (solid line; H_α) in arbitrary units.

section of the plasma is covered with 11 viewing chords. In the present study, we focus on spectra taken with the central chord. The height of the viewing area is approximately ± 5 cm from the equatorial plane and the horizontal (toroidal) extent is ± 10 cm. The latter is determined by a vertical slit located in the vacuum chamber located between the LHD port and the spectrometer.

We made observation for a discharge with the configuration of $R_{ax} = 3.63$ m and $B_{ax} = 2.7$ T, where R_{ax} and B_{ax} are the radius of the magnetic axis and the magnetic field strength at the magnetic axis, respectively. The temporal development of the discharge is shown in Fig. 1. The discharge is initiated by electron cyclotron heating and sustained with three neutral beams. Eight hydrogen pellets are sequentially injected at intervals of 40 ms starting from $t = 0.7$ s. During pellet injection, the electron density is increased stepwise and in synchrony with each pellet injection while the electron temperature is lowered. After pellet injection ends, the electron density gradually decreases and the electron temperature recovers.

Figure 2 shows the Lyman- α spectrum accumulated between $t = 1$ s and 2 s, during which the line-averaged n_e decreased from $2.5 \times 10^{20} \text{ m}^{-3}$ to $1.1 \times 10^{20} \text{ m}^{-3}$. A remarkable feature of this spectrum is the dip emerging at the line center. The fine structure and the Zeeman splitting are too small to explain the distance between the two peaks. A feasible explanation is the so-called self-reversal arising from the strong reabsorption effect. Since reabsorption of the Lyman- α line is caused by the ground state hydrogen

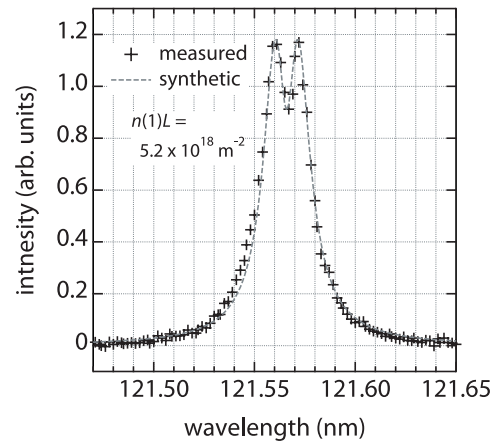


Fig. 2 Example of the observed Lyman- α line profile showing self-reversal (+). Dashed line is the result of fitting in the radiation transport analysis.

atom, the self-reversal profile should have some information concerning the atom density. In the following section, we attempt to deduce the hydrogen atom density from the observed spectral line profile.

3. Model Calculation

The simplest situation that gives rise to self-reversal in the spectral profile is the case when the photons emitted in a hot region are observed through a cold atom region that significantly absorbs the passing photons. Since the absorption profile of cold atoms is narrower than the emission profile when these profiles are determined by Doppler broadening, the absorption is more significant in the central region of the emission profile than at the edge, and thus the observed line profile could show a dip at the line center.

However, since neutral hydrogen atoms are considered to exist predominantly in a narrow layer located at the plasma edge [2], such a two layer model would be inappropriate in the present case. Instead, we consider a single layer in which emission and absorption occur simultaneously, and attempt to derive the atom density in the layer from the observed spectral profile of the Lyman- α line.

The atom layer, which is here considered as the emission and absorption medium of the Lyman- α line, is modelled by a slab of width of L . The coordinate x is taken in the direction of the thickness, and its origin is taken at the middle of the layer, i.e., $-L/2 < x < L/2$, as shown in Fig. 3.

For the energy levels of the hydrogen atom, which are related to the emission and absorption processes of the Lyman- α line, only the ground ($n = 1$) and $n = 2$ states are considered. This assumption is adequate unless the absolute line intensity or absolute excited level density is considered. The parameters T_e , n_e , and the ground state density n_1 are assumed to be constant in the medium.

The intensity of the Lyman- α line at wavelength λ and at location x is written as $I_\lambda(x)$. The derivative of $I_\lambda(x)$ with

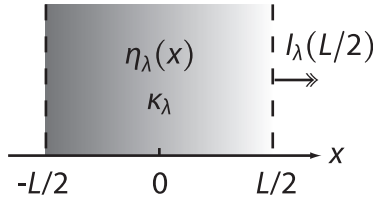


Fig. 3 Schematic view of absorption medium considered here. The absorption coefficient κ_λ is constant while the emission coefficient η_λ depends on the location x according to the $n = 2$ level population.

respect to x can be expressed as [5]

$$\frac{d}{dx}I_\lambda(x) = \eta_\lambda(x) - \kappa_\lambda(x)I_\lambda(x), \quad (1)$$

where $\eta_\lambda(x)$ and $\kappa_\lambda(x)$ are the emission and absorption coefficients, respectively. These coefficients, which are generally functions of λ and x , are explicitly written as [5]

$$\eta_\lambda = \frac{hc}{4\pi\lambda_0}n_2A(2, 1)P_\lambda, \quad (2)$$

$$\kappa_\lambda = \frac{hc}{4\pi\lambda_0}n_1B(1, 2)P_\lambda = \frac{\lambda_0^4}{2\pi c}n_1A(2, 1)P_\lambda, \quad (3)$$

where, h and c are the Planck's constant and the speed of light, respectively, n_2 is the $n = 2$ level population, and $A(2, 1)$ and $B(1, 2)$ are Einstein's A and B coefficients for the Lyman- α line, respectively. The intrinsic spectral profile P_λ , namely, the profile uninfluenced by reabsorption processes, is assumed to be common for both the η_λ and κ_λ , and to be constant in the medium. The profile P_λ is normalized as $\int P_\lambda d\lambda = 1$.

Since n_1 is assumed to be constant, κ_λ is constant as well. If n_2 or η_λ is also constant, self-reversal never appears, irrespective of the optical thickness. The spatial distribution of n_2 could indeed have a peaked profile; η_λ depends on x when the medium is optically thick for the Lyman- α line even if other parameters are constant. This point will be discussed below. We obtain the observable spectral profile, namely, that at the edge of the medium ($x = L/2$), by solving Eq. (1). The result can be written as

$$I_\lambda\left(\frac{L}{2}\right) = \int_{-L/2}^{L/2} \eta_\lambda(x) \exp\left[-\kappa_\lambda\left(\frac{L}{2} - x\right)\right] dx. \quad (4)$$

Calculation of Eq. (4) requires $n_2(x)$ which is involved in $\eta_\lambda(x)$. For evaluation of $n_2(x)$, the steady-state Holstein equation is called for. In a general three-dimensional space the distribution of the $n = 2$ level density, $n_2(\mathbf{r})$, should satisfy an equation expressed as [6]

$$E(\mathbf{r}) = A(2, 1)n_2(\mathbf{r}) - A(2, 1) \int_V n_2(\mathbf{r}')G(\mathbf{r}, \mathbf{r}')d\mathbf{r}', \quad (5)$$

where $E(\mathbf{r})$ is the excitation rate from the $n = 1$ to $n = 2$ level at location \mathbf{r} due to electron collisions in the present

Table 1 Parameters for Eq. (7) excerpted from Ref. [6].

	Gaussian	Lorentzian
d_1	0.9029	0.805
d_2	0.9603	0.7186
d_3	1.686	1.653
d_4	1.644	1.583

case, and $G(\mathbf{r}, \mathbf{r}')$ is the probability that a photon emitted at point \mathbf{r}' is reabsorbed at \mathbf{r} .

Solving Eq. (5) is generally difficult and solutions are given under several extreme conditions. For a slab geometry and for a homogeneous excitation rate in the medium, the normalized $n = 2$ population $\bar{n}_2(x)$ is approximately given as [6]

$$\bar{n}_2(x) = \frac{\zeta\pi/2}{L \sin(\zeta\pi/2)} \cos\left(\zeta\pi\frac{x}{L}\right), \quad (6)$$

where $\bar{n}_2(x)$ satisfies $\int \bar{n}_2(x)dx = 1$. The parameter ζ depends on the profile P_λ and is given as

$$\zeta = d_1 \left(\frac{\kappa_0 L + d_2}{\kappa_0 L + d_2 d_3} \right)^{d_4}, \quad (7)$$

where the constants d_1 to d_4 are shown in Table 1 for the Gaussian and Lorentzian profiles. Equation (6) is valid in the range $0 \leq \kappa_0 L \leq 1000$.

The $\bar{n}_2(x)$ profile is calculated with Eqs. (6) and (7), and with the parameters in Table 1 for the Gaussian and Lorentzian profiles as a function of $\kappa_0 L$, where κ_0 is the absorption coefficient at the line center. In both cases, more peaked profile is obtained with increasing $\kappa_0 L$ until $\kappa_0 L$ reaches 100, and in the range of $\kappa_0 L > 100$, no further changes appear in the $n_2(x)$ profile. As seen in Eqs. (2) and (4), the normalized value for $n_2(x)$ is sufficient, and no absolute density is necessary as far as the spectral profile I_λ in relative units is concerned.

4. Results and Discussion

For simplification of the analysis, Eq. (4) is rewritten and the normalized intensity profile $\bar{I}_\lambda(L/2)$ is defined as

$$\bar{I}_\lambda\left(\frac{L}{2}\right) = \mathcal{P}_\lambda \int_{-1}^1 \bar{n}_2(\xi) \exp\left[-\kappa_0 L \mathcal{P}_\lambda \frac{1-\xi}{2}\right] d\xi, \quad (8)$$

where the coordinates are changed as $\xi = x/(L/2)$, and \mathcal{P}_λ is the same as P_λ but is re-normalized to be unity at the line center, so that $\kappa_0 \mathcal{P}_\lambda = \kappa_\lambda$, and all the constant values that change only the entire magnitude of the spectrum are omitted.

When the line profiles are assumed to be Gaussian, \mathcal{P}_λ is written explicitly as

$$\mathcal{P}_\lambda = \exp\left[-\left(\frac{\lambda - \lambda_0}{\Delta\lambda_D}\right)^2\right], \quad (9)$$

where $\Delta\lambda_D$ is the half width at $1/e$ intensity. Figure 4 shows the results of Eq. (8) for several $\kappa_0 L$ values, where

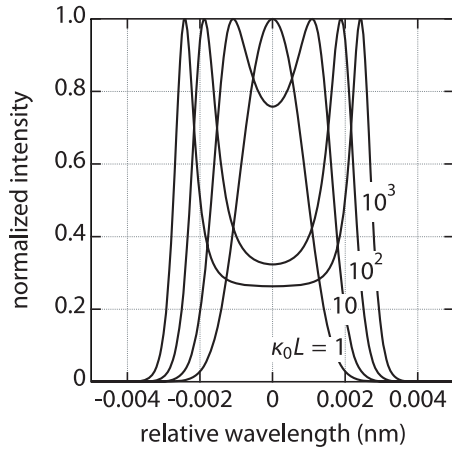


Fig. 4 Lyman- α line profiles calculated with Eqs. (8) and (9) for several $\kappa_0 L$ values, where $\lambda_0 = 0$ nm and $\Delta\lambda_D = 0.001$ nm. The magnitude is normalized so that the maximum intensity becomes unity.

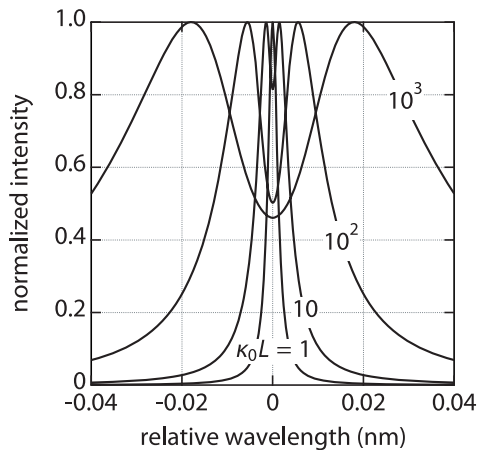


Fig. 5 Lyman- α line profiles calculated with Eqs. (8) and (10) for several $\kappa_0 L$ values, where $\lambda_0 = 0$ nm and $\gamma = 0.002$ nm. The magnitude is normalized so that the maximum intensity becomes unity.

$\Delta\lambda_D$ is fixed at 0.001 nm. For Lorentzian profiles, \mathcal{P}_λ is written as

$$\mathcal{P}_\lambda = \frac{(\gamma/2)^2}{(\lambda - \lambda_0)^2 + (\gamma/2)^2}, \quad (10)$$

where γ is the full width at half maximum. Figure 5 shows the results for several $\kappa_0 L$ values, where γ is fixed at 0.002 nm.

The measured line profile in Fig.2 is fitted with

Eq. (8), where $\kappa_0 L$ and $\Delta\lambda_D$ or γ , which depends on the profile adopted for \mathcal{P}_λ , are the fitting parameters. In the actual fitting of the measured profile, the instrumental function is convoluted for the synthetic profile, and the entire magnitude of Eq. (8) is normalized to the measured profile.

No reasonable parameters are found when Gaussian profiles are used for \mathcal{P}_λ . The best fit is obtained with a Lorentzian profile for \mathcal{P}_λ with $\gamma = 0.0018$ nm and $\kappa_0 L = 100$. The fitting result is shown with a dashed line in Fig. 2, where the synthetic profile includes the instrumental function.

Given the constant values in Eq. (3), we obtain $n_1 L = 5.2 \times 10^{18} \text{ m}^{-2}$. The result is understood as indicating, for example, that $n_1 = 5.2 \times 10^{19} \text{ m}^{-3}$ when the atom layer is 10 cm thick. This density value is about one order larger than that estimated from the gas pressure in the vacuum vessel for similar discharges. However, since the gas pressure is measured several meters away from the plasma boundary and the present result is on the plasma surface, a direct comparison is difficult.

We have assumed a slab geometry for the atom layer, which has a constant electron temperature, electron density, and ground state atom density. In the actual plasma, however, those parameters should have profiles, and radiation transport may be more complicated. For more accurate analysis of the measured results, a neutral transport code that gives a detailed atom density profile would be necessary.

It should also be noted that we have found no reasonable explanation for the result that the emission and absorption profiles are well approximated by the Lorentzian profile rather than the Gaussian profile. Since similar results have also been obtained for the Balmer series lines in the visible range measurement [2], the present result is at least consistent with our empirical knowledge.

Acknowledgement

The authors are grateful to the LHD experimental group for their support. This study was partly supported by financial aid from the LHD project (NIFS09ULPP527).

- [1] R. Katai *et al.*, Plasma Fusion Res. **2**, 014 (2007).
- [2] A. Iwamae *et al.*, Phys. Plasmas **12**, 042501 (2005).
- [3] N. Ohyabu *et al.*, Phys. Rev. Lett. **97**, 055002 (2006).
- [4] R. Katai *et al.*, Rev. Sci. Instrum. **77**, 10F307 (2006).
- [5] T. Fujimoto, *Plasma Spectroscopy* (Clarendon Press, Oxford, 2004).
- [6] A. F. Molisch *et al.*, *Radiation Trapping in Atomic Vapours* (Clarendon Press, Oxford, 1998).